Published in final edited form as:
Sci Transl Med. 2013 September 25; 5(204): 204ra131. doi:10.1126/scitranslmed.3006827.

siRNA screen for genes that affect Junín virus entry uncovers voltage-gated calcium channels as a therapeutic target

Madakasira Lavanya[1], **Christian D. Cuevas**[1], **Monica Thomas**[1], **Sara Cherry**[1,3,4], and **Susan R. Ross**[1,2,3,*]

[1]Department of Microbiology, Perelman School of Medicine, University of Pennsylvania, Philadelphia, PA 19104

[2]Abramson Cancer Center, Perelman School of Medicine, University of Pennsylvania, Philadelphia, PA 19104

[3]Institute for Immunology, Perelman School of Medicine, University of Pennsylvania, Philadelphia, PA 19104

[4]Penn Genomic Frontiers Institute, Perelman School of Medicine, University of Pennsylvania, Philadelphia, PA 19104

Abstract

New world hemorrhagic fever arenaviruses infection of humans results in 15–30% mortality. We performed a high throughput siRNA screen with Junín virus glycoprotein-pseudotyped viruses to find potential host therapeutic targets. Voltage-gated calcium channels (VGCC) subunits, for which there are FDA-approved drugs, were identified in the screen. Knockdown of VGCC subunits or treatment with channel blockers diminished Junín virus-cell fusion and entry into cells and thereby decreased infection. Gabapentin, an FDA-approved drug used to treat neuropathic pain that targets the α2δ2 subunit, inhibited infection of mice by the Candid 1 vaccine strain of the

*To whom correspondence may be addressed: 313BRBII/III, University of Pennsylvania, 421 Curie Boulevard, Philadelphia, PA 19104, Phone: 215-518-2462, FAX: 215-573-2028, rosss@mail.med.upenn.edu.

Author contributions: L.M., C.D.C. and M.T. performed the experiments; L.M., C.D.C., S.C. and S.R.R. designed the experiments and analyzed the results; L.M., C.D.C. and S.R.R. wrote the paper.

Competing interests: The authors declare no competing interests.

SUPPLEMENTARY MATERIALS

Supplementary Materials and Methods

Fig. S1. Graph of Z scores showing infection levels and DAPI staining with the two sets of siRNAs used in the primary screen.
Fig. S2. Expression validation of the 10 genes in U2OS and 293T cells.
Fig. SS3. Validation of knockdown of 10 genes by siRNAs.
Fig. SS4. Effect of siRNA knockdown of 10 genes on Machupo and MLV pseudotype infection.
Fig. S5. TfR1 function is not altered by siRNA knockdown of 10 genes.
Fig. S6. TfR1 function is not altered by siRNAs targeting VGCC subunit genes or calcium channel blocker treatment.
Fig. S7. Expression of α1S and α2δ2 subunits after siRNA transfection targeting different VGCC subunits.
Fig. S8. IC50 values and MTT assays for verapamil, nifedipine and gabapentin.
Fig. S9. Knockdown or inhibition of VGCCs decreases Lassa and LCMV pseudovirus infection.
Fig. S10. VGCC blockers inhibit an early stage of Junín pseudovirus infection.
Fig. S11. Candid 1 binds to VGCCs on mouse cells.
Fig. S12. VGCCs are important for Junín pseudovirus and Candid 1 infection of mouse cells.
Table S1. Genes identified in the siRNA screen as affecting Junín pseudovirus infection.
Table S2. Z scores of all VGCC subunit channels present in primary screen.
Table S3. Sequences of siRNAs used in secondary screen.
Table S4. Additional siRNAs used in infection assays.

virus. These findings demonstrate that VGCCs play a role in virus infection and have the potential to lead to therapeutic intervention of new world arenavirus infection.

Keywords

Junín virus; Machupo virus; arenavirus; mouse mammary tumor virus; vesicular stomatitis virus; LCMV; Lassa; murine leukemia virus; voltage-gated calcium channel; gabapentin

INTRODUCTION

The Junín, Machupo and Guanarito clade B new world hemorrhagic fever arenaviruses (NWA) are associated with outbreaks in Argentina, Bolivia and Venezuela, respectively (1). Humans become infected through direct contact with rodents or by inhalation of aerosolized rodent *excreta*, primarily during harvest season or residential infestation (2). Because they are readily transmitted by aerosols, these Category A arenaviruses are potential bioterrorism agents and are included in the list of agents in the Material Threat Determinations and Population Threat Assessment issued by the Department of Homeland Security (3). Although an effective Junín virus vaccine has greatly decreased disease incidence, there are sporadic cases of this as well as the other known and novel clade B arenaviruses (4–6). Ribavirin is currently the only anti-viral drug in use for therapeutic or post-infection prophylactic treatment of arenavirus infection, although it has mixed efficacy and serious side effects in some individuals (7, 8). As such, there is a great need for the development of new anti-arenavirus therapeutics.

Arenaviruses are enveloped RNA viruses whose entry is mediated by the viral glycoproteins GP1 and GP2. Whereas old world arenaviruses like Lassa or lymphocytic choriomeningitis virus (LCMV) use cell surface α-dystroglycan for cellular entry, clade B NWAs use transferrin receptor 1 (TfR1) (9). Other viruses, such as the retrovirus mouse mammary tumor virus (MMTV) also use TfR1 as entry receptors (10). Little is known about the steps subsequent to NWA GP interaction with TfR1 on the cell surface except that fusion occurs at pH 5, suggesting that trafficking to a late endosomal/lysosomal compartment is required for entry (11–15).

Small molecule screens targeting NWA virion proteins have unveiled promising lead drug targets, but these are not yet used therapeutically (16–19). Because RNA viruses have high mutation rates, virus escape mutants to such therapies may arise. An alternative approach to the development of therapeutics directed at viral genes is to target host factors that affect infection. To this end, siRNA screens have identified novel factors not previously implicated in infection by several viruses, but not arenaviruses (20–24).

Here, a siRNA screen with Junín GP-pseudotyped retroviral vectors to identify host factors involved in NWA entry uncovered voltage-gated calcium channels (VGCCs) as pro-viral genes. Importantly, VGCC inhibitors effectively inhibited NWA infection in culture and administration of gabapentin, which specifically blocks the α2δ2 subunit, decreased Candid 1 infection of mice either after systemic or intracranial inoculation of virus. The discovery of host factors that enhance or inhibit NWA infection contributes to our understanding about

the biology of virus entry and potentially identifies new host targets for therapeutic intervention.

RESULTS

RNAi screen identifies both anti- and pro-Junín virus host genes

Arrays of 4 independent siRNAs targeting ~9,000 genes grouped in a 2 × 2 pool format were transfected into human U2OS cells. Seventy-two hr post-transfection, the cells were infected with MLV-lacZ pseudotypes bearing the Junín Parodi strain GP (25). Forty-eight hr post-infection, the cells were stained with anti-lacZ antibody and DAPI, subjected to automated image analysis and the number of cells and % infection was analyzed for each well (Fig. 1A). Candidate genes were selected that modulated infection by a Z score of >1.5 or ≤1.5 in both plates, which approximates a >2 standard deviation difference from the mean (>50% difference in virus infection) ($p \leq 0.001$; Fig. S1). Toxic siRNAs were excluded based upon decreased cell viability as measured by a robust Z score ≤2 (>30% decrease in cell number; Fig. S1 and Table S1). Knockdown controls siRNAs for lacZ and TfR1 included on the screening plates reduced infection by 6- and 2-fold (av. Z scores of −3.74and −2.22), respectively (Fig. 1B).

Hits were scored for siRNAs showing the same phenotype on both plates, representing at least 2 different siRNAs, one from each pool (26). One hundred and two genes were identified that altered Junín pseudovirus infection (Fig. 1C). Eighty-nine genes were pro-viral (knockdown decreased infection) and 13 anti-viral (knockdown increased infection) (Fig. 1C and Table S1). Molecular function (GO) analysis showed that the genes were enriched in transmembrane proteins, macromolecule localization, nucleotide binding, and voltage-gated channel activity (Fig. 1D).

Three additional independent siRNAs targeting 96 of the 102 genes were tested with Junín pseudotypes to confirm the primary screen (Fig. 1C); 26 hits were validated (≥1 siRNAs in the secondary screen affected infection). The relatively low 25% validation rate is likely due to the use of unvalidated siRNAs in both the primary and secondary analyses, as well as cell toxicity effects associated with transfection of some of the siRNAs (Table S1). Of these 26 hits, 10 affected only Junín but not VSV pseudotype infection (Fig. 1C and Table S1).

Ten genes were analyzed further (Table S1). To ensure that the siRNAs were not having off-target effects, gene expression in U2OS cells was validated by real time PCR (Fig. S2A) and in an additional human cell line, 293T (Fig.S2B); all the genes showed the same Junín and VSV pseudotype infection phenotype in U2OS and 293T cells when knocked down (see below). We also showed that siRNAs that diminished the gene's RNA levels affected infection, while siRNAs that did not decrease the RNA levels had no effect on infection (Fig. S3A).

For subsequent analyses, pseudoviruses encoding the firefly luciferase gene were used, as well as additional independent gene-specific siRNAs (Fig. S3B and Methods); cell viability was analyzed in parallel using MTT assays (Fig. S3C).

Several genes affect entry by NWAs but not other viruses

Seven of the 10 genes altered infection by Junín and VSV pseudotypes (*ARFRP1, CLDN2, CSDC2, DHX15, KSR2, LTBP2* and *SSU72*) (Fig. 1C). Junín virus and VSV enter cells through acidic endosomes and this pathway might involve genes in common. Additionally, the 7 genes could work at a post-entry step affecting MLV uncoating, reverse transcription, genome integration or transcription. We thus examined infection of 293T-MCAT1 cells by MLV Env pseudotypes, which moreover enter cells through non-acidic pathways. MMTV pseudotype infection of U2OS cells stably expressing mouse TfR1 was also tested. While human TfR1 but not mouse TfR1 serves as the entry receptor for Junín virus, the converse is true for MMTV (10, 27). We also tested whether knockdown of these genes altered Machupo virus pseudotype infection, another NWA that uses human TfR1 for entry.

Three classes of genes were identified: those that had the same effect on infection by all the pseudoviruses (*ARFRP1, CLDN2, CSDC2, DHX15, KSR2, LTBP2* and SSU72), those that altered Junín, Machupo and MMTV pseudovirus infection (*CACNA2D2* and *TRIM11*) and *TRIM2*, whose knockdown uniquely decreased infection by Junín and Machupo pseudoviruses (Fig. 2A; Fig. S4). siRNAs that targeted mouse or human TfR1 decreased MMTV or Machupo and Junín pseudovirus infection, respectively, but not VSV or MLV pseudovirus infection (Fig. 2A; Fig. S4A and B).

To determine whether the 10 genes also altered infection by replication-competent NWAs, we tested siRNA treatment on Candid 1 infection. Infection was measured by RT-qPCR with primers to the viral nucleoprotein (NP) gene to determine viral RNA levels; siRNAs that targeted TfR1 and NP served as controls. With the exception of DHX15, all the siRNAs showed an identical effect on Candid 1 and Junín pseudovirus infection (Fig. 2B). Knockdown of DHX15 increased Junín, Machupo, VSV, and MMTV pseudovirus infection but not Candid 1 or MLV pseudovirus infection (Fig. 2A and 2B, Fig. S4A and 4B).

Next, the effect of knockdown of the 10 genes on cell surface TfR1 expression and its ability to transport transferrin (Tf) were tested. While a TfR1-specific siRNA significantly decreased surface expression, TfR1 expression was not altered by siRNA treatment with any of the 11 genes (Fig. 2C). Similarly, while TfR1 knockdown decreased the ability of cells to internalize FITC-labeled Tf by about 2-fold, siRNAs targeting of the 12 genes had little or no effect on uptake (Fig. S5A). Thus, none of the genes that alter Junín virus infection play a role in TfR1's normal cellular function.

Voltage-gated calcium channels are important for Junín virus entry

CACNA2D2 encodes an α2δ2 subunit of VGCCs. VGCCs mediate the influx of calcium ions into neurons and muscle cells upon membrane polarization, and are composed of 4 subunits: α1, a 24 transmembrane-spanning domain protein constituting the channel pore, α2δ2 subunit, a polyprotein which is cleaved to make a single subunit with a glycosylated α2 domain disulfide-bonded to the δ2 membrane domain, a cytosolic β signaling subunit and γ, another multi-membrane spanning protein (28). The α2δ2, β and γ proteins function as auxiliary subunits modulating the activity of the α1 pore (28). While VGCC channel proteins are expressed in many cell types at low levels, their function in non-neuronal or -

muscle cells is not well-established. There are multiple genes for each subunit encoded in the genome.

In addition to *CACNA2D2*, *CACNB3*, encoding a β subunit, scored significantly as required for infection in the primary screen (Table S1), as well as with 1/3 independent siRNAs in the secondary screen (Fig. 1C). Several other α1 subunit genes including *CACNA1S*, and additional α2δ2 and γ subunit genes scored as pro-viral hits in 1 well of the primary screen as well (Table S2). To determine whether it was the α2δ2 subunit alone or the VGCC that was required for Junín virus and MMTV entry, siRNAs to deplete expression of α1s and β3 were tested for their effect on infection by Junín, MMTV and VSV pseudotypes and Candid1. While VSV was not affected, both Junín and MMTV pseudovirus, as well as Candid 1 infection were significantly decreased by knockdown of the subunit genes (Fig. 3A and Fig. 3B). Knockdown of the different VGCC subunits had no effect on Tf uptake (Fig. S4). However, siRNA knockdown of *CACNA2D2* and *CACNB3* decreased surface expression of the α1S subunit (Fig. S5A), and knockdown of *CACNA1S* and *CACNB3* decreased *CACNA2D2* protein levels (Fig. S5B), confirming that surface expression of the different subunits is co-dependent even in non-neuronal cells.

Calcium channel inhibitors block Junín virus entry

There is a large body of evidence implicating Ca^{2+} uptake and virus infection (29). To determine whether the decrease in Junín virus infection was the result of altered Ca^{2+} uptake or to direct effects on the channel proteins, several drugs were tested for their ability to inhibit infection by Junín GP, MMTV Env and VSV G pseudotypes, including the intra-cellular calcium chelator BAPTA-AM and L-type VGCC antagonists. The VGCC inhibitors nifedipine and verapamil, which target the α1S subunit, decreased infection by Junín and MMTV pseudotypes but not VSV, with IC50s of 4.08μM and 2.03μM, respectively (Figs. 3C and S6). Neither BAPTA-AM nor the control ester BCECF-AM had an effect on infection (Fig. 3C). U73122, which inhibits phospholipase C, affects intra-cellular Ca2+ signaling and receptor-mediated phosphinositol turnover, inhibited Junín and MMTV but not VSV pseudovirus infection while its negative control, U73343 did not. Identical results were obtained for Candid 1 infection (Fig. 3D).

Gabapentin, which belongs to a class of drugs specific for the α2δ2 subunit that are widely used to treat neuropathic pain and epilepsy (30), was also tested. Gabapentin inhibited infection Junín GP and MMTV Env pseudotypes and Candid 1 but not VSV G pseudotypes (IC50 = 0.19mM) (Fig. 3C and 3D; Fig. S6). Gabapentin, verapamil and nifedipine had no effect on Tf uptake or on TfR1 expression (Fig. S4). The VGCC inhibitors as well as VGCC siRNA treatment inhibited infection by pseudotypes bearing the Lassa and LCMV GPs, old world arenaviruses that use α-dystroglycan for entry, albeit to a lesser extent (Fig. S7).

VGCCs function at an early stage in Junín virus infection

That knockdown and inhibition of VGCCs decreased infection by both replication-competent Candid 1 and Junín pseudoviruses suggested that the channel was playing a role in entry. To determine when the VGCCs were functioning, we compared the kinetics of verapamil inhibition to that of the vacuolar-type H+-ATPase inhibitor bafilomycin A (bafA).

Pre-treatment of U2OS cells with bafA dramatically decreased Junín pseudovirus infection, even when removed at 30 min post-infection (Fig. S8). Addition of bafA up to 30 min post-infection also significantly decreased virus infection; when added 1 hr post-infection, the drug had no effect (Fig. S8), demonstrating that virus entry into the cell from a low pH compartment occurred within 1 hr after addition of virus to cells. We then carried out the same kinetic experiment with verapamil. Similar to what was seen with bafA, addition of verapamil prior to and during but not 30 min post-infection decreased Junín pseudovirus infection (Fig. S8A). Neither verapamil nor bafA affected infection by MLV Env pseudoviruses (Fig. S8B).

We next tested the role of VGCCs in virus binding to cells. FITC-labeled Candid 1 was bound to human and mouse cells pre-treated with the siRNAs to *TFR1* and *CACNA1S*. While treatment with the *CACNA1S* siRNA alone did not alter the amount of virus bound to human cells, bound virus was significantly decreased in cells co-transduced with siRNAs to both *TFR1* and *CACNA1S* or *CACNA2D2* compared to *TFR1* alone (Fig. 4A). Knockdown of *CACNA1S* or *CACNA2D2* but not mouse *TFR1* in mouse cells also decreased binding (Fig. S11A); mouse TfR1 does not bind NWAs (27).

We also tested whether virus binding decreased surface expression of the receptors. When human cells were incubated with Candid 1, there was a significant reduction in the surface expression of both α1S and TfR1 but not major histocompatibility class I (MHC-I) (Fig. 4B); this effect was specific for Candid 1, since incubation with VSV pseudotypes had no effect. Incubation of mouse cells with Candid 1 decreased α1S surface expression while having no effect on mouse TfR1 levels (Fig. S11B).

To test if VGCCs were required for efficient virus-cell fusion, we used syncytia-induction as a surrogate assay. Expression of the Junín virus GP on the cell surface leads to syncytia formation at pH5 but not pH7 (31, 32). Mouse cells were treated with siRNAs targeting *TFR1*, *CACNA1S* or *CACNA2D2*, transiently transfected with a Junín GP expression construct and then pulsed at pH5 or pH7. The cells transfected with the VGCC subunit siRNAs showed significantly smaller syncytia (fewer nuclei/syncytium), as well as fewer syncytia (Fig. 5A and 5B). Syncytia-induction was not dependent on TfR1 since it occurred in mouse cells (Fig. 5A) and *TFR1* knockdown had no effect. Similar results were obtained with gabapentin- or verapamil-treated cells, whereas genistein, which inhibits Junín infection by blocking a signaling step in infection (33), had no effect (Fig. 5C). Collectively, these data suggest that virus binds to VGCCs and that this interaction plays a role in virus entry at the virus-cell fusion step.

Gabapentin blocks Junín virus infection *in vivo*

We next tested whether VGCCs were required for infection of mice. Junín virus can infect mouse cells via a TfR1-independent mechanism, albeit inefficiently compared to human cells (32, 34). Knockdown of *CACNA1S* or *CACNA2D2* greatly decreased infection of mouse macrophage cells by both Junín and MMTV pseudotypes (Fig. S12A) and gabapentin treatment inhibited Candid 1 infection (Fig. S12B). In contrast, only MMTV and not Junín infection was affected by *TFR1* knockdown (Fig. S12A), as we previously reported (32).

We then tested the effect of gabapentin in mice. Mice can be infected systemically (35, 36) or intracranially (37) with pathogenic Junín virus; moreover, the Candid 1 vaccine strain was generated by extensive passaging after injection into newborn mouse brains (38). Four week old mice were given an intravenous injection of different amounts of gabapentin followed by intra-peritoneal inoculation with 1×10^6 pfu of Candid 1; mice received the same daily dose of drug until sacrifice at 1 week pi. With doses as low as 10μg/g body weight, gabapentin significantly reduced viral RNA levels and titers (Fig. 6B and C). Similar results were obtained after intra-cranial injection of newborn mice with Candid 1 and administration of the indicated doses of gabapentin via intra-peritoneal injection. Gabapentin treatment had a dramatic effect on virus RNA levels (Fig. 6C) and virus titers in the brains of treated mice (Fig. 6D); several had titers 10^4-fold lower than the average untreated mouse. Importantly, gabapentin blocked *in vivo* infection of mice using either route of administration when given at doses well below the maximum tolerated dose in humans (up to 3600 mg/day). Thus, VGCCs are also critical for Junín virus infection *in vivo* and may serve as a therapeutic target.

Discussion

Rodent-borne arenaviruses remain an important human health concern. The NWAs cause hemorrhagic fever in humans with about 30% mortality (2) while the old world arenavirus, Lassa virus found in western Africa, infects 300,000–500,000 individuals annually, with approximately 5,000 deaths (39). With the exception of Junín virus, there are no vaccines available for preventative or prophylactic treatment of infection by these viruses and ribavirin, which has only limited efficacy, is the only anti-viral therapeutic currently in use. Here, using Junín GP-pseudotyped MLV cores, we show that siRNA screening for host genes involved in arenavirus infection can successfully lead to the identification of new cellular targets for therapeutic intervention.

Only 100 genes passed our initial stringent validation criteria, and of these, only 29 were validated with additional siRNAs. Indeed, even *TFR1* did not score as a pro-viral hit in the screen. We believe that the low number of identified genes is due to the use of pooled, unvalidated siRNAs in the library that either do not “hit” or sufficiently decrease expression of their targets; additionally, there are on- and off-target effects on cell viability. This is supported by our finding that some siRNAs to some of the VGCC channel genes, such as *CACNA1S* decreased infection in 1 of the 2 screening plates.

We identified several genes that affected infection by all the pseudotypes as well as by the Junín vaccine strain Candid 1, including *ARFRP1, CLDN2, CSDC2, KSR2, LTBP2* and *SSU72*. These host genes may play a general role in entry by enveloped viruses and thus represent additional promising targets for the development of pan-anti-viral therapies. One gene, *DHX15*, uniquely affected infection by the pseudoviruses but not Candid 1. *DHX15*, which encodes a DEAH box-containing ATP-dependent RNA helicase with roles in both spliceosome and ribosome biosynthesis, has the potential to alter host gene expression through either its role in splicing or translation (40, 41). Its knockdown could result in differential effects on one-hit pseudovirus and replication-competent arenavirus infection.

TRIM2 was found to be anti-viral only for the NWAs. *TRIM2* is a ubiquitin ligase belonging to a gene family that includes a large number of viral restriction factors (42). *TRIM2* is highly expressed in neuronal cells and is believed to play a role in cellular polarization by ubiquitination of neurofilament light chains (43). However, it is also expressed at low levels in other cell types, including as shown here, U20S and 293T cells as well as in other tissues (44). Another member of the TRIM family found in the screen, *TRIM11*, was pro-viral for infection by Junín virus and MMTV; this factor has also neuronal cell function (45) and was previously shown to enhance MLV entry by interfering with the Ref1 restriction factor (42). Further studies on the how these different factors affect NWA infection, as well as infection by retroviruses, are currently in progress.

Importantly, the VGCC channel protein genes *CACNA1S*, *CACNA2D2* and *CACNB3* were identified in the screen as necessary for efficient infection by Junín virus. Because of the co-dependence of the different VGCC subunits on their expression on the cell surface, our studies do not distinguish whether it is the VGCC or a particular subunit that is required for efficient Junín virus infection. However, we showed that VGCCs likely play an early role in the infection pathway: their cell-surface expression increases virus binding to cells, they are co-downregulated with TfR1 when bound to virus and they are required for efficient pH5-dependent virus GP-mediated cell fusion. In contrast, knockdown or pharmacological inhibition did not apparently alter TfR1 expression or function, indicating that the two receptors do not interact, at least in the absence of virus. Our data suggest that the channel proteins are involved in the initial steps of virus entry, perhaps by serving as co-receptors for entry.

Several studies have shown that there is low-level infection by NWAs on murine cells and those from other species whose TfR1 does not bind NWAs (11, 27, 32, 34). Our data suggest that VGCCs are important for the low-level TfR1-independent infection seen in mice and may function as entry receptors in this species. Our data may explain how the Candid 1 vaccine was able to be generated by passage through newborn mouse brains without using murine TfR1 for entry (38). Interestingly, about 10% of individuals infected with NWAs experience neurological symptoms which may be in part because VGCCs are highly expressed on neuronal cells, although the origin of the neuropathology has not been definitively linked to direct virus infection or specific histopathology (2).

The requirement for VGCCs led us to test well-known drugs that target these channels for their effect on infection, and indeed, verapamil, nifedipine and gabapentin all efficiently inhibited infection by both Junín pseudoviruses and the Candid 1 vaccine strain in cell lines. Although nifedipine, verapamil and gabapentin are known to affect decrease cellular calcium levels by decreasing its uptake, this did not appear to play a role in inhibiting virus infection as is the case for other viruses such as enteroviruses (46), since the Ca^{2+} chelator BAPTA-AM had no effect on infection. We do not yet know how nifedipine and verapamil, which bind the α1s subunit or gabapentin, which binds the α2δ2 subunit, alter VGCC/virus interaction, although given the negative effect on virus-cell fusion, this likely occurs through drug-induced structural changes in the receptor that prevent virus binding (47, 48). Interestingly, down-modulation of VGCCs by siRNAs or drugs also decreased infection by MMTV pseudotypes, which also use TfR1 for entry, as well as to a lesser extent by LCMV

or Lassa pseudotypes, which do not. Further work is required to determine if the effects for these viruses are via the same or a different entry mechanism than we found for Junín virus.

Gabapentin was effective in reducing Candid 1 infection in an *in vivo* mouse model. While these data are promising in identifying new potential therapeutics for treatment of NWAs, we have only demonstrated *in vivo* gabapentin efficacy with the Junín virus vaccine strain and in an animal model that does not support pathogenic infection. Further studies treating pathogenic Junín virus infection in guinea pigs, the small animal model which best mimics human pathogenesis, are currently planned.

While the Junín virus vaccine has greatly decreased disease incidence in Argentina, sporadic cases of infection still occur in endemic areas. Moreover, there are other clade B viruses, such as Machupo virus, and new members that are frequently discovered, for which there are no vaccines or good therapeutics (6). Our finding that VGCCs are important for NWA entry and that commonly used drugs that target the channel proteins block infection by Junín virus, suggests an effective off-label use of VGCC blockers in the treatment of NWA infection.

METHODS

Study design

This study used automated high throughput siRNA library screening as a first step in the identification of genes that enhanced (pro-viral) or inhibited (anti-viral) infection by Junín virus. After using stringent criteria for gene selection from the primary screen, they were subjected first to secondary automated screening using different siRNAs and then to a series of cell-based assays to determine their specificity for NWAs versus other viruses, if any were feasible therapeutic targets. Details regarding sampling and experimental replicates for these assays are included in the figure legends.

Cells and pseudoviruses

U2OS (human osteosarcoma) and MCAT1-293T (49) cells were cultured in Dulbecco's Modified Eagle Medium (DMEM) supplemented with 10% fetal bovine serum (FBS); the media for the latter was supplemented with 5 μg/ml geneticin (Invitrogen). NMuMG (normal murine mammary gland) epithelial cells (ATCC) were cultured in DMEM/10% FBS/10μg/ml insulin. NR-9456 mouse macrophages (NIAID/NIH BEI Research Resources Repository) were cultured in the presence of sodium pyruvate. 293T cells were transiently transfected with pHIT60 (MLV Gag-pol encoding plasmid), pHIT111/pFB luciferase (MLV genome harboring either lacZ/luciferase reporter gene), and expression vectors containing the respective viral glycoprotein gene (Junín GP, Machupo GP, MMTV Env, VSVG, MLV Env, Lassa GP, LCMV GP) (10, 25, 50–52). Pseudotypes were harvested at 48h post-transfection, filtered through 0.45μM filters (Millipore) and stored at −80°C. When required, pseudovirus was concentrated on Amicon Centrifuge columns (Amicon, Inc.).

High-Throughput Screening

The Ambion druggable genome RNAi library containing siRNAs targeting human genes was used for the screen. siRNAs were spotted on black, clear bottom 384 well plates (Corning). Set one (plates 1–27) contained 2 siRNAs per well, set 2 (plates 28–54) contained two different siRNAs per well for the same gene. Reverse transfection with Hiperfect transfecting reagent (Qiagen) was used to transfect the siRNAs. 72h after knockdown, the cells were infected with Junín-pseudotyped MLV virus with a Lac-Z reporter gene and 48h post-infection stained with rabbit Anti-Lac Z antibody (Cappel, Inc.) followed by anti-rabbit Alexa488 (Invitrogen) and DAPI (Sigma). The plates were imaged using ImageXpress Micro (Molecular Devices) with a 20× objective. Three images were acquired per well in both the DAPI and 488 nm channels. The percentages of infected and DAPI-positive cells were calculated using automated image analysis software (MetaXpress, Leica). The percent infection was log transformed to calculate Z-scores for each well. “Hits” were identified as those wells that exhibited a change in infection (increase or decrease) by ≥1.5 standard deviations from average Z –score for the entire plate. Toxic siRNAs were excluded based upon decreased cell viability as measured by a Z-score ≤2 which corresponds to a decrease in cell number of more than 30%. Each plate also included siRNAs to human transferrin receptor (Dharmacon), lacZ (Invitrogen) and siDeath (Qiagen). After the primary screen, 99 of the 102 genes that scored as hits were re-tested with 3 independent siRNAs (Qiagen, Inc.) (Table S3). Additional siRNAs were used for knockdown assays with luciferase viruses and Candid 1 (Table S4). TFRC siRNAs (Ontarget Smart Pool; Thermo Scientific, Inc.) were used in all the assays.

Candid 1 infection

Candid 1 was propagated in Vero cells. siRNA-transduced U2OS cells were seeded in 96 well plates and infected with Candid 1 (MOI 0.1/cell). Residual, unattached virus was washed off with PBS and DMEM supplemented with 2% FBS. RNA was harvested at 24 hr pi and analyzed by reverse transcribed real-time qPCR. Candid 1 RNA was analyzed by RT-qPCR, as previously described (32). All assays were performed in triplicate and each assay was performed at least 3 times.

Luciferase assays

Cells were infected with pseudoviruses containing the luciferase reporter gene in a 96 well format. At 24 hr pi, the cells were incubated with the Britelite plus (Perkin Elmer) substrate for 5 min. Luciferase activity was measured using an automated plate reader (Molecular Devices). All assays were performed in triplicate and each assay was performed at least 3 times.

CACNA1S and surface TfR1 levels

U2OS cells were transfected with the indicated VGCC subunit siRNAs. Seventy two hour post-transfection cells were harvested with PBS/1mM EDTA and stained with mouse anti-dihydropyridine binding complex (α1s) antibody (Millipore). Cells were washed with PBS/2% FBS/0.01% sodium azide and stained with Alexa488-conjugated secondary

antibody. TfR1 levels were determined by FACS using human anti-CD71-PE or -FITC (Invitrogen).

RNA isolation and RT-qPCR

Cells were washed with RNALater reagent (Ambion) and total RNA was isolated using RNeasy kit (Qiagen). cDNA was synthesized using Qiagen Reverse transcript kit. RNAs were analyzed by reverse-transcribed real-time quantitative PCR (RT-qPCR) using a 7800HT sequence detector system (Applied Biosystems) with the indicated primer pairs. All RT-qPCR reactions were performed using a Power SYBR green PCR kit (Applied Biosystems). All RNA amplifications were normalized to glyceraldehyde-3-phosphate dehydrogenase (GAPDH). The fold change in RNA was calculated by the delta-delta CT method.

Inhibitors

U73122 (25μM; Enzo), U73343 (10μM; Enzo), BCECF-AM (10μM; Invitrogen), BAPTA-AM (10μM; Invitrogen), gabapentin (500 μM; Sigma), nifedipine (10μM; Sigma) and verapamil (10μM; Sigma), were diluted in DMEM and cells were pretreated for 1h or 5h (for gabapentin) at 37°C prior to and during infection with the pseudoviruses or Candid1. After 18 hr the media was replaced without inhibitors, unless otherwise indicated. Virus infection was assayed at 48 hr post-infection. MTT assays were performed to ensure that inhibitors were not cytotoxic to cells at the concentrations used (Fig. S7).

Binding assay using FITC labeled Candid1

Candid 1 was concentrated by centrifugation on 30% sucrose cushions, titered and labeled with FITC using Fluorotag FITC conjugation kit (Sigma). Cells were pretreated with inhibitors or transfected with siRNAs and incubated with FITC-labeled Candid 1 for 1 hr on ice and then transferred to 37°C for 1h; a particle/cell ratio of 1000 was used to ensure saturation of all binding sites. Cells were detached using PBS/1mM EDTA and resuspended in PBS containing 2% FBS/0.01% sodium azide. Cells were analyzed by FACS (FACSCalibur; Becton Dickinson) using FlowJO (Tree Star, Inc.) software.

Syncytia assay

NMuMG cells were reverse transfected with siRNAs using Lipofectamine RNAiMax reagent (Invitrogen) or treated with VGCC inhibitors as described above. Twenty four hr later, the cells were transfected with the Junín virus GP expression vector, using Lipofectamine LTX reagent (Invitrogen). After 48hr, the cells were pulsed for 5 minutes with citrate buffer (pH 5 or pH 7), refed with fresh medium and incubated overnight at 37°C. The cells were fixed with methanol and stained with Giemsa (Sigma, Inc.). The number of syncytia and number of nuclei in each syncytium were scored across 20 different fields in each of 4 experiments. The data are presented as the % relative to the control siRNA-treated cells.

Mice

Mice were housed according to the policies of the Institutional Animal Care and Use Committee of the University of Pennsylvania and all experiments were approved by this committee. C57BL/6 mice were purchased from the Jackson Laboratory and were housed and bred at Penn under ABSL2 conditions. Six or 8 day old pups were treated with gabapentin (100 μg/g) via intraperitoneal inoculation. One hr after gabapentin treatment, the mice were injected with Candid 1 (1×10^4 pfu; 20–30 μl) by intracranial injection into the left brain hemisphere using a 28G ½ in needle. The pups initially treated with gabapentin received additional doses at 2, 3 and 4 dpi. Mice were sacrificed at 5 dpi and the left brain hemisphere was collected. The brain was homogenized by douncing with the plunger of an insulin syringe (Becton Dickinson) and then centrifuged for 10 min, 8000 rpm at 4°C. The supernatant was used to titer Candid 1 by plaque assay as described previously (32). RNALater reagent (Ambion) was added to the brain homogenate and total RNA was isolated using Trizol (Ambion). For systemic infections, 4 week old mice received intravenous injections of 10, 100 or 500μg/g gabapentin (Hi-tech Pharmacon). One hour after treatment, mice were inoculated intraperitoneally with JUNV Candid1 (1×10^6 pfu) in no more than 1ml with a 27G ½ in needle. Daily gabapentin treatments at the same doses were administered intraperitoneally. At one week post-infection mice were sacrificed and the spleens were homogenized by douncing and centrifuged to generate a cell pellet and supernatant. The supernatants were titered on Vero cells and RNA was isolated from the pellet using RNeasy kits (Qiagen, Inc.).

Statistical Analysis

Statistical analysis was done using Prism software. Methods used to calculate p values are described in the figure legends.

Supplementary Material

Refer to Web version on PubMed Central for supplementary material.

Acknowledgments

We thank Robert Tesh for Candid 1, Lorraine Albritton for the MCAT1-293T cell line, Paula Cannon, Mike Farzan, Michael Buchmeier and James Cunningham for constructs and Carolyn Coyne and Kevin Foskett for advice on the inhibitor studies. NR-9456 cells were obtained through the NIH Biodefense and Emerging Infections Research Resources Repository, NIAID, NIH.

Funding: Supported by MARCE U54-AI-057168, by the University of Pennsylvania Transdisciplinary Program in Translational Medicine and Therapeutics and by the Penn Genome Frontiers Institute, which is funded in part by a grant from the Pennsylvania Department of Health. C.D.C. was supported by PHS T32-AI-055400 and M. Thomas by PHS R25-HL-084665.

References

1. Charrel RN, de Lamballerie X. Arenaviruses other than Lassa virus. Antiviral Res. 2003; 57:89–100. [PubMed: 12615305]
2. Gomez RM, Jaquenod de Giusti C, Sanchez Vallduvi MM, Frik J, Ferrer MF, Schattner M. Junin virus. A XXI century update. Microbes Infect. 2011; 13:303–311. [PubMed: 21238601]

3. HHS Public Health Emergency Medical Countermeasure Enterprise Implementation Plan for Chemical, Biological, Radiological, and Nuclear Threats. 2007
4. Enria DA, Briggiler AM, Sanchez Z. Treatment of Argentine hemorrhagic fever. Antiviral Res. 2008; 78:132–139. [PubMed: 18054395]
5. Aguilar PV, Camargo W, Vargas J, Guevara C, Roca Y, Felices V, Laguna-Torres VA, Tesh R, Ksiazek TG, Kochel TJ. Reemergence of Bolivian hemorrhagic fever, 2007–2008. Emerg Infect Dis. 2009; 15:1526–1528. [PubMed: 19788833]
6. Delgado S, Erickson BR, Agudo R, Blair PJ, Vallejo E, Albarino CG, Vargas J, Comer JA, Rollin PE, Ksiazek TG, Olson JG, Nichol ST. Chapare virus, a newly discovered arenavirus isolated from a fatal hemorrhagic fever case in Bolivia. PLoS Pathog. 2008; 4:e1000047. [PubMed: 18421377]
7. Charrel RN, Coutard B, Baronti C, Canard B, Nougairede A, Frangeul A, Morin B, Jamal S, Schmidt CL, Hilgenfeld R, Klempa B, de Lamballerie X. Arenaviruses and hantaviruses: from epidemiology and genomics to antivirals. Antiviral Res. 2011; 90:102–114. [PubMed: 21356244]
8. McCormick JB, King IJ, Webb PA, Scribner CL, Craven RB, Johnson KM, Elliott LH, Belmont-Williams R. Lassa fever. Effective therapy with ribavirin. The New England journal of medicine. 1986; 314:20–26. [PubMed: 3940312]
9. Choe H, Jemielity S, Abraham J, Radoshitzky SR, Farzan M. Transferrin receptor 1 in the zoonosis and pathogenesis of New World hemorrhagic fever arenaviruses. Curr Opin Microbiol. 2011; 14:1–7. [PubMed: 21239215]
10. Ross SR, Schofield JJ, Farr CJ, Bucan M. Mouse transferrin receptor 1 is the cell entry receptor for mouse mammary tumor virus. Proc. Natl. Acad. Sci. USA. 2002; 99:12386–12390. [PubMed: 12218182]
11. Oldenburg J, Reignier T, Flanagan ML, Hamilton GA, Cannon PM. Differences in tropism and pH dependence for glycoproteins from the Clade B1 arenaviruses: implications for receptor usage and pathogenicity. Virology. 2007; 364:132–139. [PubMed: 17397892]
12. Castilla V, Palermo LM, Coto CE. Involvement of vacuolar proton ATPase in Junin virus multiplication. Arch. Virol. 2001; 146:251–263. [PubMed: 11315636]
13. York J, Nunberg JH. Role of the stable signal peptide of Junin arenavirus envelope glycoprotein in pH-dependent membrane fusion. J. Virol. 2006; 80:7775–7780. [PubMed: 16840359]
14. Wang E, Obeng-Adjei N, Ying Q, Meertens L, Dragic T, Davey RA, Ross SR. Mouse mammary tumor virus uses mouse but not human transferrin receptor 1 to reach a low pH compartment and infect cells. Virology. 2008; 381:230–240. [PubMed: 18829060]
15. Martinez MG, Cordo SM, Candurra NA. Characterization of Junin arenavirus cell entry. The Journal of general virology. 2007; 88:1776–1784. [PubMed: 17485539]
16. Lee AM, Rojek JM, Spiropoulou CF, Gundersen AT, Jin W, Shaginian A, York J, Nunberg JH, Boger DL, Oldstone MB, Kunz S. Unique small molecule entry inhibitors of hemorrhagic fever arenaviruses. J Biol Chem. 2008; 283:18734–18742. [PubMed: 18474596]
17. Thomas CJ, Casquilho-Gray HE, York J, DeCamp DL, Dai D, Petrilli EB, Boger DL, Slayden RA, Amberg SM, Sprang SR, Nunberg JH. A specific interaction of small molecule entry inhibitors with the envelope glycoprotein complex of the Junin hemorrhagic fever arenavirus. J Biol Chem. 2011; 286:6192–6200. [PubMed: 21159779]
18. Urata S, Yun N, Pasquato A, Paessler S, Kunz S, de la Torre JC. Antiviral activity of a small-molecule inhibitor of arenavirus glycoprotein processing by the cellular site 1 protease. J Virol. 2011; 85:795–803. [PubMed: 21068251]
19. Larson RA, Dai D, Hosack VT, Tan Y, Bolken TC, Hruby DE, Amberg SM. Identification of a broad-spectrum arenavirus entry inhibitor. J Virol. 2008; 82:10768–10775. [PubMed: 18715909]
20. Krishnan MN, Ng A, Sukumaran B, Gilfoy FD, Uchil PD, Sultana H, Brass AL, Adametz R, Tsui M, Qian F, Montgomery RR, Lev S, Mason PW, Koski RA, Elledge SJ, Xavier RJ, Agaisse H, Fikrig E. RNA interference screen for human genes associated with West Nile virus infection. Nature. 2008; 455:242–245. [PubMed: 18690214]
21. Brass AL, Dykxhoorn DM, Benita Y, Yan N, Engelman A, Xavier RJ, Lieberman J, Elledge SJ. Identification of host proteins required for HIV infection through a functional genomic screen. Science. 2008; 319:921–926. [PubMed: 18187620]

22. Li Q, Brass AL, Ng A, Hu Z, Xavier RJ, Liang TJ, Elledge SJ. A genome-wide genetic screen for host factors required for hepatitis C virus propagation. Proc Natl Acad Sci U S A. 2009; 106:16410–16415. [PubMed: 19717417]
23. Konig R, Zhou Y, Elleder D, Diamond TL, Bonamy GM, Irelan JT, Chiang CY, Tu BP, De Jesus PD, Lilley CE, Seidel S, Opaluch AM, Caldwell JS, Weitzman MD, Kuhen KL, Bandyopadhyay S, Ideker T, Orth AP, Miraglia LJ, Bushman FD, Young JA, Chanda SK. Global analysis of host-pathogen interactions that regulate early-stage HIV-1 replication. Cell. 2008; 135:49–60. [PubMed: 18854154]
24. Panda D, Das A, Dinh PX, Subramaniam S, Nayak D, Barrows NJ, Pearson JL, Thompson J, Kelly DL, Ladunga I, Pattnaik AK. RNAi screening reveals requirement for host cell secretory pathway in infection by diverse families of negative-strand RNA viruses. Proc Natl Acad Sci U S A. 2011; 108:19036–19041. [PubMed: 22065774]
25. Reignier T, Oldenburg J, Noble B, Lamb E, Romanowski V, Buchmeier MJ, Cannon PM. Receptor use by pathogenic arenaviruses. Virology. 2006; 353:111–120. [PubMed: 16797051]
26. Echeverri CJ, Beachy PA, Baum B, Boutros M, Buchholz F, Chanda SK, Downward J, Ellenberg J, Fraser AG, Hacohen N, Hahn WC, Jackson AL, Kiger A, Linsley PS, Lum L, Ma Y, Mathey-Prevot B, Root DE, Sabatini DM, Taipale J, Perrimon N, Bernards R. Minimizing the risk of reporting false positives in large-scale RNAi screens. Nat Methods. 2006; 3:777–779. [PubMed: 16990807]
27. Radoshitzky SR, Kuhn JH, Spiropoulou CF, Albarino CG, Nguyen DP, Salazar-Bravo J, Dorfman T, Lee AS, Wang E, Ross SR, Choe H, Farzan M. Receptor determinants of zoonotic transmission of New World hemorrhagic fever arenaviruses. Proc Natl Acad Sci U S A. 2008; 105:2664–2669. [PubMed: 18268337]
28. Catterall WA. Voltage-gated calcium channels. Cold Spring Harb Perspect Biol. 2011; 3:a003947. [PubMed: 21746798]
29. Zhou Y, Frey TK, Yang JJ. Viral calciomics: interplays between Ca2+ and virus. Cell Calcium. 2009; 46:1–17. [PubMed: 19535138]
30. Davies A, Hendrich J, Van Minh AT, Wratten J, Douglas L, Dolphin AC. Functional biology of the alpha(2)delta subunits of voltage-gated calcium channels. Trends Pharmacol Sci. 2007; 28:220–228. [PubMed: 17403543]
31. Castilla V, Mersich SE. Low-pH-induced fusion of Vero cells infected with Junin virus. Archives of virology. 1996; 141:1307–1317. [PubMed: 8774689]
32. Cuevas CD, Lavanya M, Wang E, Ross SR. Junin virus infects mouse cells and induces innate immune responses. J Virol. 2011; 85:11058–11068. [PubMed: 21880772]
33. Vela EM, Bowick GC, Herzog NK, Aronson JF. Genistein treatment of cells inhibits arenavirus infection. Antiviral Res. 2008; 77:153–156. [PubMed: 17961732]
34. Flanagan ML, Oldenburg J, Reignier T, Holt N, Hamilton GA, Martin VK, Cannon PM. New World Clade B arenaviruses can use transferrin receptor 1 (TfR1)-dependent and - independent entry pathways, and glycoproteins from human pathogenic strains are associated with the use of TfR1. J. Virol. 2008; 82:938–948. [PubMed: 18003730]
35. Mettler NE, Casals J. Susceptibility of mice aged 0–14 days to infection with Junin virus. Proceedings of the Society for Experimental Biology and Medicine. Society for Experimental Biology and Medicine. 1970; 134:1051–1054.
36. Kolokoltsova OA, Yun NE, Poussard AL, Smith JK, Smith JN, Salazar M, Walker A, Tseng CT, Aronson JF, Paessler S. Mice lacking alpha/beta and gamma interferon receptors are susceptible to junin virus infection. J Virol. 2010; 84:13063–13067. [PubMed: 20926559]
37. Lascano EF, Berria MI. Immunoperoxidase study of astrocytic reaction in Junin virus encephalomyelitis of mice. Acta Neuropathol. 1983; 59:183–190. [PubMed: 6303038]
38. Albarino CG, Ghiringhelli PD, Posik DM, Lozano ME, Ambrosio AM, Sanchez A, Romanowski V. Molecular characterization of attenuated Junin virus strains. J. Gen. Virol. 1997; 78:1605–1610. [PubMed: 9225036]
39. Ogbu O, Ajuluchukwu E, Uneke CJ. Lassa fever in West African sub-region: an overview. J Vector Borne Dis. 2007; 44:1–11. [PubMed: 17378212]

40. Arenas JE, Abelson JN. Prp43: An RNA helicase-like factor involved in spliceosome disassembly. Proc Natl Acad Sci U S A. 1997; 94:11798–11802. [PubMed: 9342317]
41. Combs DJ, Nagel RJ, Ares M Jr, Stevens SW. Prp43p is a DEAH-box spliceosome disassembly factor essential for ribosome biogenesis. Mol Cell Biol. 2006; 26:523–534. [PubMed: 16382144]
42. Uchil PD, Quinlan BD, Chan WT, Luna JM, Mothes W. TRIM E3 ligases interfere with early and late stages of the retroviral life cycle. PLoS Pathog. 2008; 4:e16. [PubMed: 18248090]
43. Balastik M, Ferraguti F, Pires-da Silva A, Lee TH, Alvarez-Bolado G, Lu KP, Gruss P. Deficiency in ubiquitin ligase TRIM2 causes accumulation of neurofilament light chain and neurodegeneration. Proc Natl Acad Sci U S A. 2008; 105:12016–12021. [PubMed: 18687884]
44. Wu C, Orozco C, Boyer J, Leglise M, Goodale J, Batalov S, Hodge CL, Haase J, Janes J, Huss JW 3rd, Su AI. BioGPS: an extensible and customizable portal for querying and organizing gene annotation resources. Genome Biol. 2009; 10:R130. [PubMed: 19919682]
45. Tuoc TC, Stoykova A. Trim11 modulates the function of neurogenic transcription factor Pax6 through ubiquitin-proteosome system. Genes Dev. 2008; 22:1972–1986. [PubMed: 18628401]
46. Coyne CB, Bozym R, Morosky SA, Hanna SL, Mukherjee A, Tudor M, Kim KS, Cherry S. Comparative RNAi screening reveals host factors involved in enterovirus infection of polarized endothelial monolayers. Cell Host Microbe. 2011; 9:70–82. [PubMed: 21238948]
47. Kang MG, Felix R, Campbell KP. Long-term regulation of voltage-gated Ca(2+) channels by gabapentin. FEBS letters. 2002; 528:177–182. [PubMed: 12297300]
48. Striessnig J, Grabner M, Mitterdorfer J, Hering S, Sinnegger MJ, Glossmann H. Structural basis of drug binding to L Ca2+ channels. Trends in pharmacological sciences. 1998; 19:108–115. [PubMed: 9584627]
49. Zavorotinskaya T, Qian Z, Franks J, Albritton LM. A point mutation in the binding subunit of a retroviral envelope protein arrests virus entry at hemifusion. J. Virol. 2004; 78:473–481. [PubMed: 14671127]
50. Soneoka Y, Cannon PM, Ramsdale EE, Griffiths JC, Romano G, Kingsman SM, Kingsman AJ. A transient three-plasmid expression system for the production of high titer retroviral vectors. Nucl. Acids Res. 1995; 23:628–633. [PubMed: 7899083]
51. Radoshitzky SR, Abraham J, Spiropoulou CF, Kuhn JH, Nguyen D, Li W, Nagel J, Schmidt PJ, Nunberg JH, Andrews NC, Farzan M, Choe H. Transferrin receptor 1 is a cellular receptor for New World haemorrhagic fever arenaviruses. Nature. 2007; 446:92–96. [PubMed: 17287727]
52. Buchmeier MJ, Southern PJ, Parekh BS, Wooddell MK, Oldstone MB. Site-specific antibodies define a cleavage site conserved among arenavirus GP-C glycoproteins. J Virol. 1987; 61:982–985. [PubMed: 3546729]

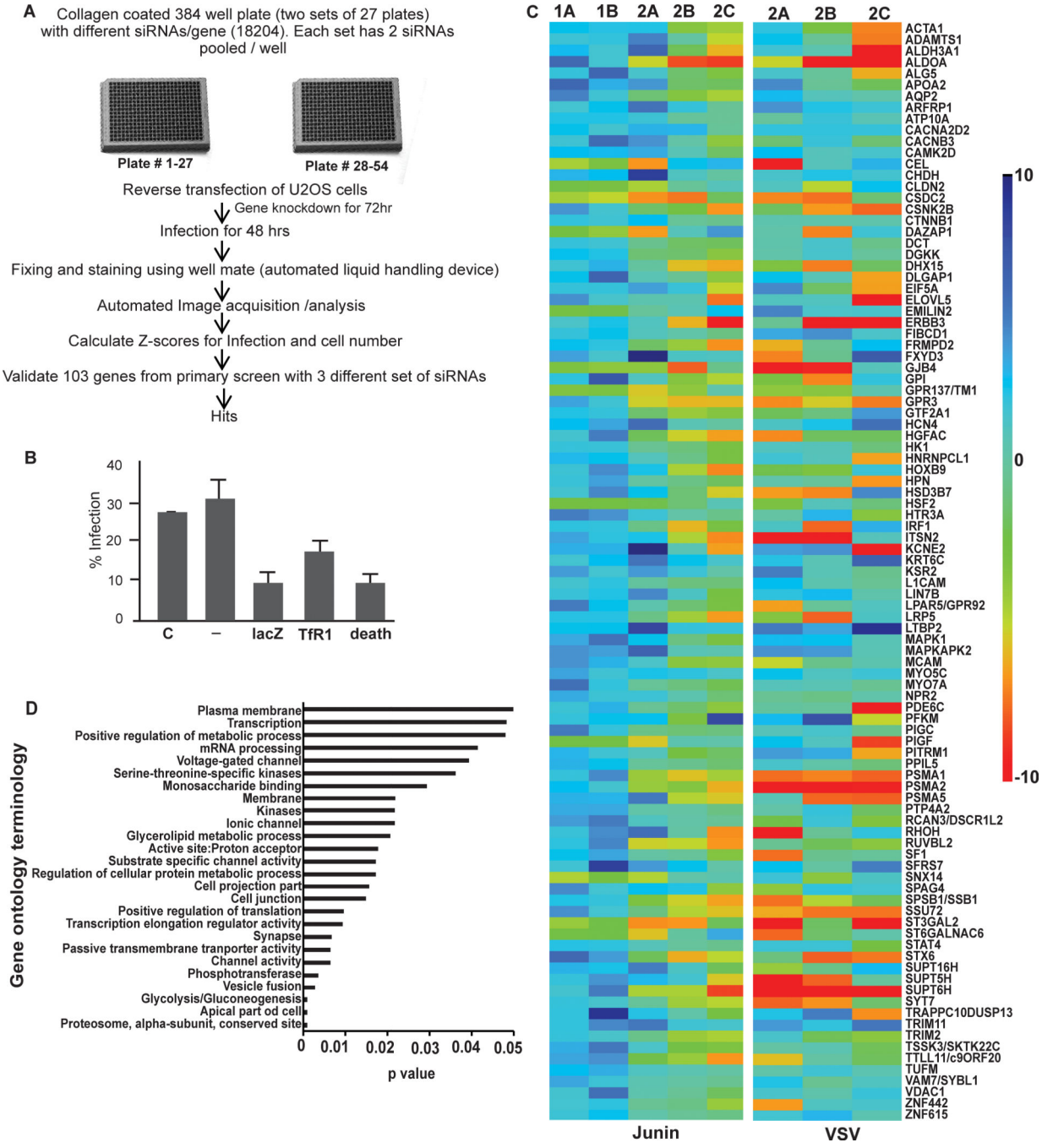

Fig. 1.

High throughput siRNA screening results. (a) Schematic representation of screen. (b) Representative infection levels from the 384 well screen plates that were transfected with siRNAs targeting the reporter (lacZ), the entry receptor (TfR1), random siRNA control (C) or no siRNA (−). The transfection efficiency on each plate was monitored using siRNA death (death). (c) Heat map of infection Z-scores for 96 genes identified in the Junín primary (1A, 1B) and secondary screen (2A, 2B, 2C), and VSV with siRNAs from the secondary screen. Blue indicates decrease in infection and red indicates increase in infection. (d) Gene

ontology biological process terms significantly ($p \leq 0.05$) overrepresented by the 96 genes that scored in the primary screen.

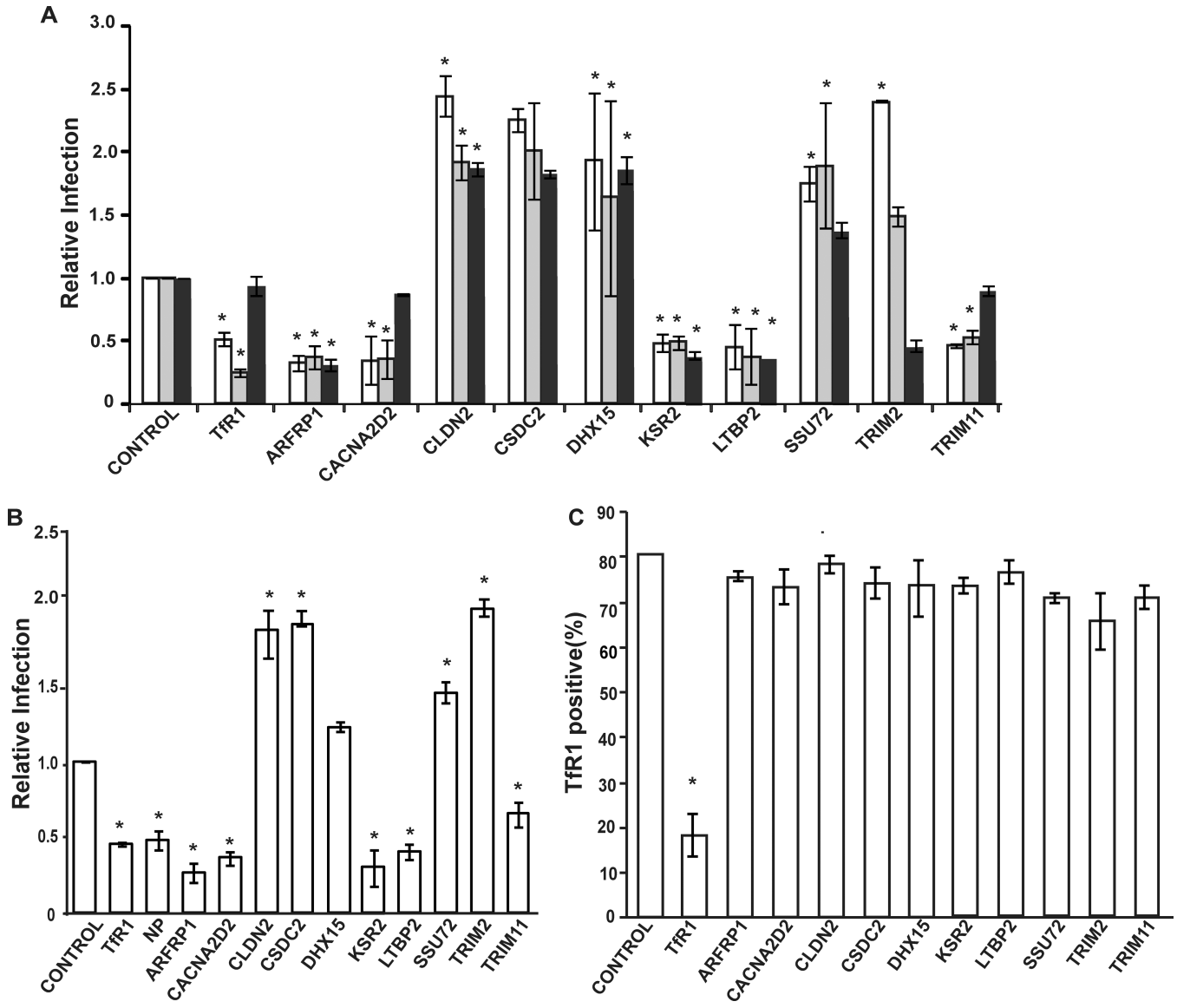

Fig. 2.

Gene knockdown effects on Junín pseudovirus or Candid 1 infection and TfR1 levels. (a) The indicated siRNAs were transfected into U2OS stably expressing mouse TfR1 receptor and infected with MLV-pseudotyped with the Junín (open bars), MMTV (grey) or VSV (black) glycoproteins. Infection levels were measured by luciferase assays; values are normalized to the control siRNA to calculate relative infection. Data present the mean ± SD of three independent experiments. (b) U2OS cells were transfected with indicated siRNAs and 72h post-transfection, challenged with Candid 1. Quantitative RT-PCR for the expression of Junín NP was analyzed 24 hpi; a siRNA targeting the NP served as a control. Data present the mean ± SD of three independent experiments. (c) Surface TfR1 (CD71) levels were quantified in U2OS cells after 72h post-siRNA transfection by FACS. A siRNA targeted to *TFR1* was used as a control. This experiment was performed twice with similar results. Statistical significance was determined by one way (b) or two way (a) ANOVA. *, $p \leq 0.05$.

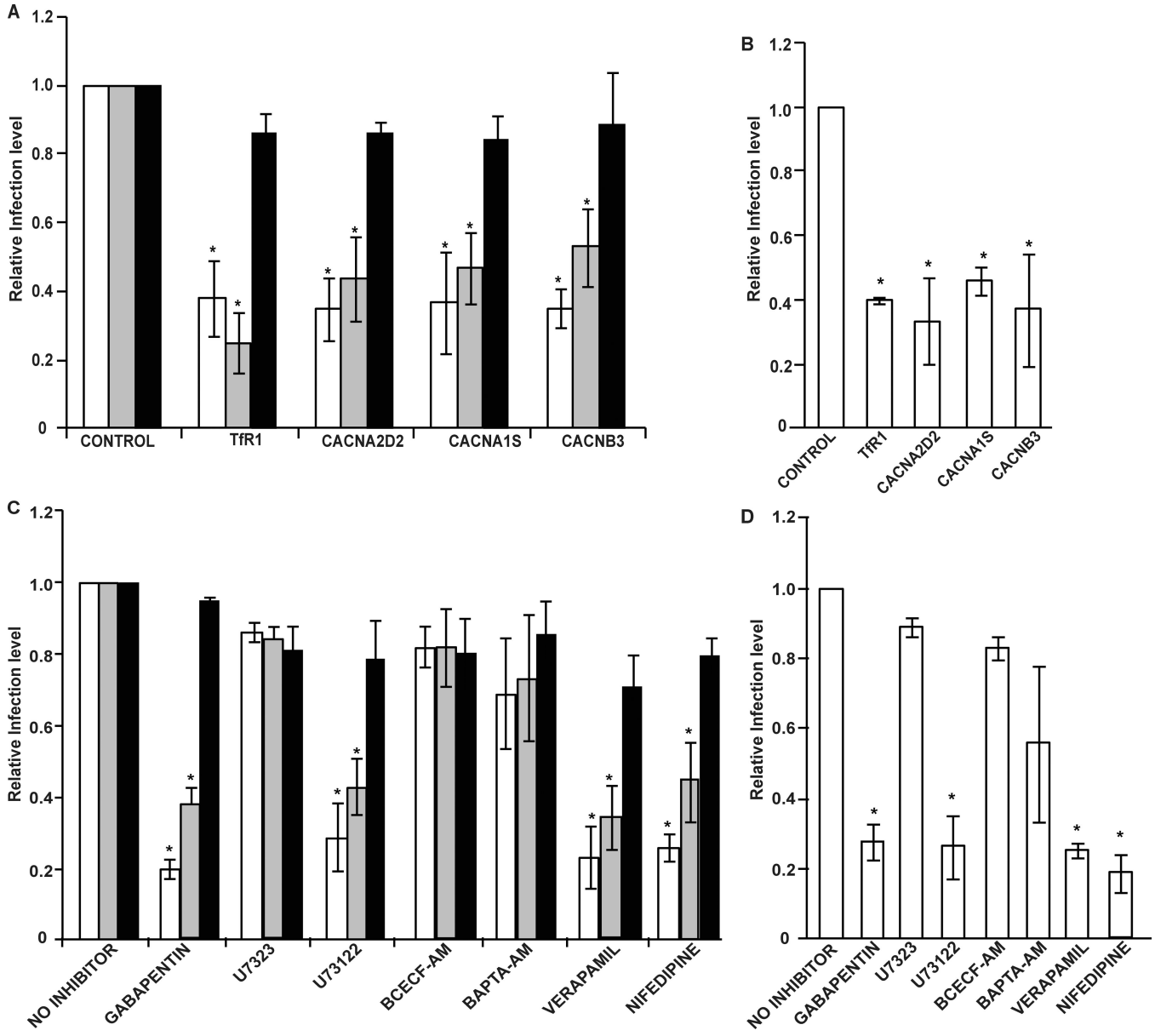

Fig. 3.

VGCCs are required for efficient infection by Junín virus and MMTV. (a) siRNAs that target the different calcium channel subunits as indicated were transfected into U2OS stably expressing the mouse TfR1 receptor. Cells were infected with Junín-(open bars), MMTV-(grey bars) or VSV-(black bars) pseudotyped virus. (b) U2OS cells were transfected with indicated siRNAs and challenged with Candid virus for 24h. RT-qPCR for the expression of Junín NP was analyzed. (c) U2OS cells stably expressing mouse TfR1 receptor were pre-incubated for 1h with indicated inhibitor, except gabapentin (5 hr pre-incubation). Cells were infected with indicated pseudovirus and luciferase activity was assayed. (d) U2OS cells were pretreated with the indicated Inhibitors and infected with Candid. Reverse transcribed RT-qPCR for the NP was analyzed. All graphs show the mean ± SD of three independent

experiments. Statistical significance was determined by one- (b, d) or two-way (a, c) ANOVA. *, $p \leq 0.05$.

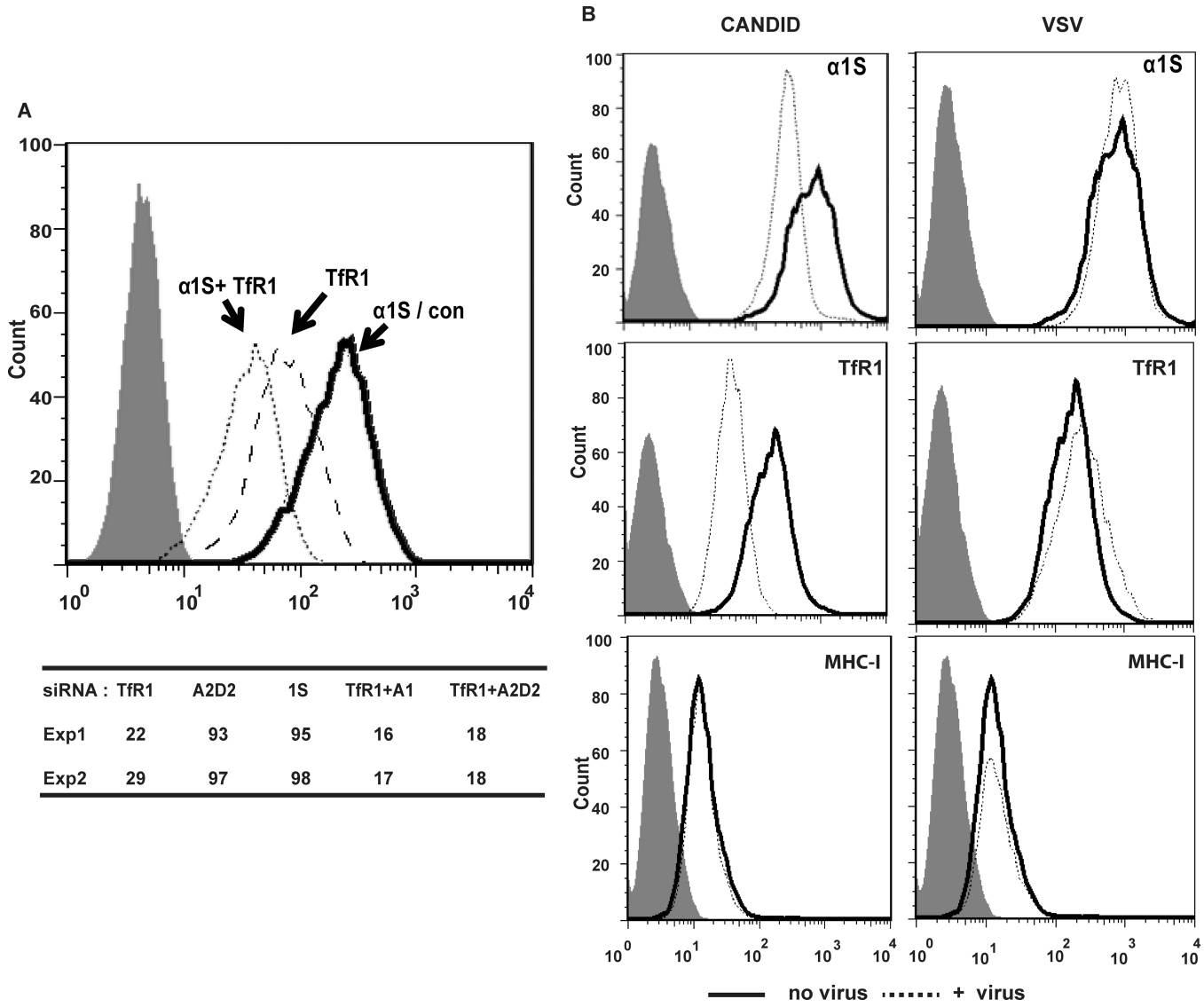

siRNA :	TfR1	A2D2	1S	TfR1+A1	TfR1+A2D2
Exp1	22	93	95	16	18
Exp2	29	97	98	17	18

Fig. 4.

Interaction of Candid 1 with VGCC subunits on the cell surface. (a) Cells treated with the indicated siRNAs and incubated with FITC-labeled Candid 1. Shown is a representative FACs plot and below the graph, the average MFI of the peaks averaged from 2 independent experiments. (b) Candid 1 or VSV pseudoviruses were incubated on ice for 30 min and then shifted to 37C for 1 hr. Cells were stained with anti-α1S, -TfR1 and –MHC Class I antibodies and analyzed by FACS.

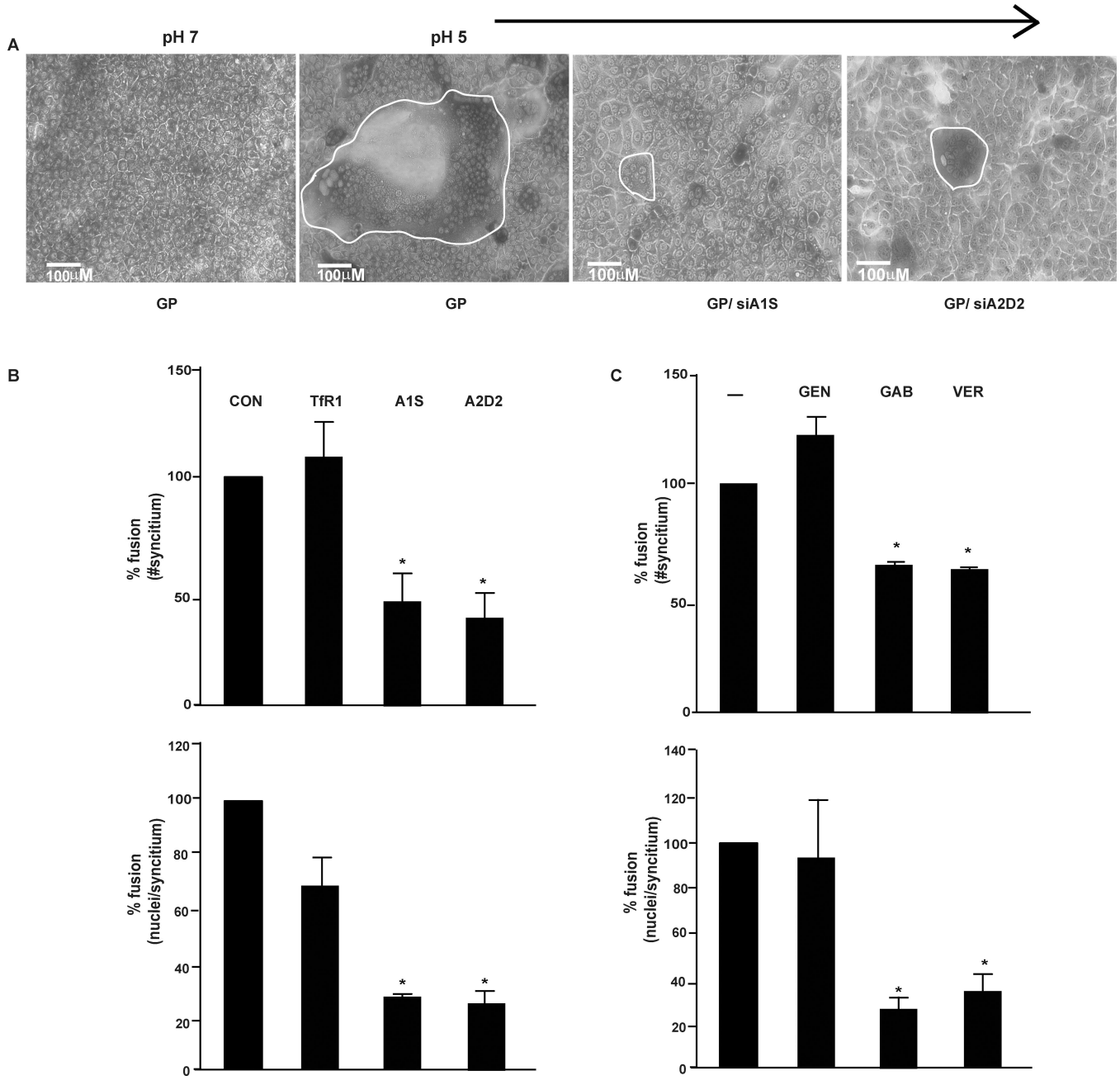

Fig. 5.

VGCCs are required for virus-cell fusion. (a) NMuMG cells were transfected with the indicated siRNAs, transfected with a Junín GP expression vector and subjected to a pH7 or pH5 pulse. Syncytia are circled in white. (b) The number of syncytia (top) and number of nuclei/syncytium (bottom) in cells transfected with *TFR1*, *CACNA1S* or *CACNA2D2* siRNAs relative to the siControl-transfected cells. Values represent the mean ± SD of 4 independent experiments. (c) Syncytia-induction in cells treated with the indicated drugs relative to untreated cells. Abbreviations: GEN, genistein; GAB, gabapentin; VER,

verapamil. Values represent the mean ± SD in 3 independent experiments. Statistical significance was determined by one way ANOVA. *, p≤0.05.

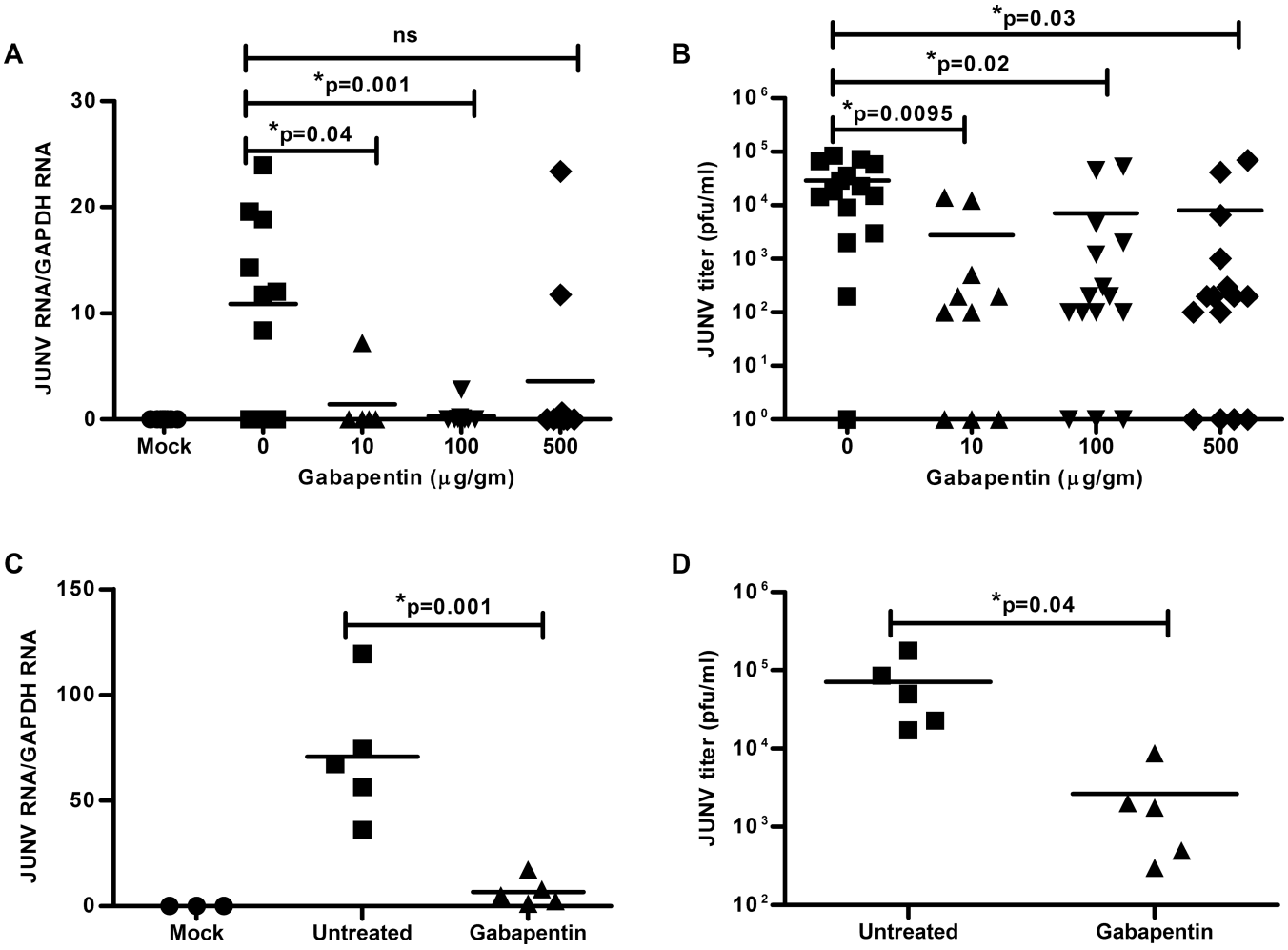

Fig. 6.

Gabapentin blocks Candid 1 infection of mice. (a) Junín NP RNA detected by reverse-transcribed RT-qPCR mice inoculated systemically with Candid 1 and treated with the indicated amounts of gabapentin. Two mice treated with 500 μg/g produced virus; these mice likely did not receive an adequate dose of gabapentin by tail vein injection because the large volume administered caused rupture of the vein. (b) Candid 1 titers in the spleens of gabapentin-treated mice. (c) Junín NP RNA in the brains of gabapentin-treated mice infected with Candid 1 by intra-cranial inoculation. (d) Candid 1 titers in the brains of treated mice. Two experiments where 4 (6-day) and 5 (8-day) mice were used for each condition. Statistical analysis was done using a double-tailed Student's T-test using an error cutoff of p = 0.05. P values for the different comparisons are indicated above the graphs.